Romanian Reports in Physics, Vol. 59, No. 4, P. 1173–1192, 2007

Dedicated to Prof. Dumitru Barbu Ion's 70th Anniversary

α-HALFLIVES OF THE GROUND AND EXCITED STATES OF HEAVIEST ELEMENTS

I. SILIȘTEANU[1], A. NEACȘU, A. O. SILIȘTEANU, M. RIZEA

Horia Hulubei Institute of Physics and Nuclear Engineering
RO-077125, Bucharest-Magurele, Romania
E-mail: silist@theory.nipne.ro

(Received August 17, 2007)

Abstract. The development of the microscopic theory of α decay is reviewed and detailed, formulas applying to heaviest nuclides are presented. A quantitative shell model theory is formulated within the famework of the multichannel resonance scattering approach. Results are presented from new calculations on ground-ground or ground-rotational-band α-decay patterns for heaviest nuclei with $Z = 104–118$. From a coupled channel analysis of decay rates the spectroscopic information on the nuclear structure of the decaying state is obatained. Particular emphasis is given to the resonance spectroscopy with position-sensitive charge particle detectors, since high-precision calculation of partial widths of narrow resonances have become now available and the resonances near the thresholds can now be observed in experiments. The reliability of the present results is demonstrated through a comparison between the decay data and relevant theories or other approaches.

Key words: reaction theory; superheavy elements, alpha-decay; resonance tunneling; valence nucleons.

PACS numbers: 25.70.Jj; 27.90.+b

1. INTRODUCTION

A central theme through the history of experimental nuclear physics has been the pursuit of nuclei at the extremes. These extremes, be they in terms of mass, proton-to-neutron ratio, or excitation energy and spin, provide impetus to develop and exploit new facilities, instrumentation and methods. The only successful methods for the laboratory synthesis of new superheavy elements (SHEs) have been fusion-evaporation reactions using heavy-element targets, heavy projectiles and fast and efficient on-line recoil separators. In many of these reactions there have been detected channels of decay which matched very well the signature expected for the nuclear decay of a superheavy nucleus. Both the

[1] Corresponding author.

quality and quantity of the experimental data on the properties of nuclear-energy levels and nuclear decay modes of the heaviest nuclei have increased over the last decade.

As nuclei move further from β stability on the proton rich side, their binding energy rapidly decreases, due to increasing Coulomb repulsion and reaction *Q*-values, which leads to major difficulties in their production and also in the study of their decay properties. The relatively large *Q*-values cause high excitations in nuclear systems involved and open up many competing decay channels favouring the nuclei closer to stability. Damping these excitations can be very crucial for nuclei produced near the limit of proton stability. The classical fission barriers of the heaviest elements with $Z > 100$ approache zero because of the large Coulomb energy. A large shell correction energy leads to additional binding and, hence, creates a sizable fission barrier of up to 8 MeV. However, a series of measurements have established that the elements with *Z* up to 118 are sufficiently bound against fission to preferentially decay by α-emission. Currently, all of the knowledge about the properties of the SHEs is based on the observation of α-decay and spontaneous fission.

Significant progress in the experimental SHE research raised a natural question of how to gain access to the basic ground-state properties of these nuclei – their masses, liftimes, momenta, spins and radii. This involves developing and applying theories and methods of prediction, analysis and interpretation of specific data, with the aim of achieving a deeper understanding of the physical nature of many quantum nucleon systems. The progress made thus far in such theories and the availability of faster and larger computers, enable us to investigate the nuclear properties of new SHEs.

The heaviest nuclei far from closed shell are expected to be deformed, which leads to the observation of several α-particle groups with similar energies, *i.e.*, fine structure, and this may reveal important additional information on nuclear structure. The stability of SHEs connected to the shape and deformation can be studied in terms of two of the most important typical structures (TS) in nuclei, which are the clustering and fine structure. The stability of nuclei depends strongly on shell structure effects and increases significantly at closed proton and neutron shells. The experimental signatures of TS have been traditionally strong and are supported by selective excitation in α-decay and transfer reactions, rotational and vibrational spaced energy levels, enhanced transition strengths and intensities, and appreciable emission width for the resonant states above the decay threshold. Progress in obtaining the most complete information on the development of TS in heaviest nuclei is being made on several fronts:

1) Improving the structure models in order to describe essential features and obtain spectroscopic information that can then be tested against data.

2) Extending the range of applicability of reaction models by using accurate reaction channels methods (including antisymmetrisation, deformation, resonance scattering, etc).
3) Including microscopic fine structure information in the coupled channel reaction models.

Using the basic ingredients of all these models and methods, we report here the first systematic study of decay rates in the classic α-decay theory, focussing on their dependence of the reaction amplitude on the microscopic (shell model) formation amplitude. In this article we accurately calculate the absolute α-emission rates for resonances in spherical and axially deformed fields. We develop a method to obtain scattering wave functions in the vicinity of a multichannal resonance on the real axis, by solving the radial Schrödinger equation for coupled channels with outgoing asymptotics and resonance conditions. Our main purpose in this work is to involve the current nuclear structure models in microscopic estimations of preformation factors in order to obtain accurate predictions for the α-decay rates in agreement with existing data.

In Section 2 we present the basic formulas for calculating the emission rates in the single channel and many channel cases. In Section 2.1 we stress some of the resonance features of the single channel solution that we shall require for the extension, in Section 2.2 to the resonance solution in the many-channel case. The resonance solution of systems of coupled equations is obtained by a direct numerical integration using step-by-step methods on computer. Some variants of the Gordon and Numerow methods are found to be most efficient for these problems. Applications are given in Sect. 3 for the α-decay of deformed superheavy elements (SHE). Section 4 compares our results with previous ones and recent data. Concluding remarks are made in Section 5.

2. AN OUTLINE OF THE THEORY

There are many theoretical approaches in the literature to α-decay of SHEs but it is rather dificult to decide which theory or what combination of theories should be used for the most significant interpretation of the experimental data. The first microscopic description of α-decay was an application of a general theory of nuclear reactions, the *R*-matrix theory [1, 2]. This, combined with the shell model, which was introduced at the same time, opened the possibility of performing microscopic calculations for the nucleon clustering into the α-particle and its subsequent emission [3–5]. The *R*-matrix width contains the channel radius parameter, which is an arbitrary parameter and often interpreted as a disadvantage of the theory. To overcome this disadvantage, in the dynamical reaction theories [6, 7] there have been formulated alternative approximations [8–11] which are

reviewed in [22]. The dominant feature of many reaction processes in which two nuclei collide at low energies to form a compound nucleus, which subsequently disintegrates in a pair of nuclei, is the appearance of resonances [15–17]. The characteristic common to all these approximations is the employment of quasistationary resonance levels and the competition between the different modes of disintegrations. The experimental observation of resonances has a great importance in reactions with heavy ions since they are sharp they may be interpreted as levels of reaction product and since such connection contributes directly to decay and in-beam studies of nuclear structure. In many cases the experimental result is usually clear to indicate the position of level and its width to draw some conclusions regarding the size of the system or the internal normalization of the wave function if it is adjusted to give the unit flux at an infinite distance.

From a mathematical point of view, the problems of Gamow states defined as eigenstates of the time independent Schrödinger equation with purely outgoing boundary, are very similar to those of the continuum shell model for nucleons [15]. In both cases, the usual quantum mechanical rules for normalizations, orthogonality and completeness have to be extended in order to take into account the bound as well as the scattering wave functions in a straightforward manner. The complex eigenvalue solutions of the Schrödinger equation give the positions of the resonance states as well as their lifetimes. A description of the resonance phenomena via complex eigenvalue solutions has the advantage of containing stationary structures as well as dynamical coupling effects.

It is the aim of the present paper to extend the developments [12, 17–19] in order to study the radioactive decay properties of nuclei at the limits of stability.

3. DECAY OF A RESONANCE LEVEL

3.1. SINGLE CHANNEL

In the simplest case of α-decay of a single resonance state k into a single decay channel n, the decay width is [13]:

$$\Gamma_n^k = 2\pi \left| \frac{\int_{r_{\min}}^{r_{\max}} I_n^k(r) u_n^0(r) dr}{\int_{r_{\min}}^{r_{\max}} I_n^k(r) u_n^k(r) dr} \right|^2 \tag{1}$$

where $I_n^k(r)$ is the particle (cluster) formation amplitude (FA) and $u_n^k(r)$ and $u_n^0(r)$ are the solutions of the system of differential equations:

$$\left[\frac{\hbar^2}{2m}\left(\frac{d^2}{dr^2}-\frac{l_n(l_n+1)}{r^2}\right)-V_n(r)+Q_n\right]u_n^0(r)=0 \tag{2}$$

$$\left[\frac{\hbar^2}{2m}\left(\frac{d^2}{dr^2}-\frac{l(l+1)}{r^2}\right)-V_n(r)+Q_n\right]u_n^k(r)=I_n^k(r) \tag{3}$$

The radial functions in Eqs. (2) and (3) describe the radial motion of the fragments at large and small separations, respectively by using the reduced mass m, the kinetic energy of emitted particle $Q_n = E - E_T - E_P$, the FA $I_n^k(r)$, l_n are the angular momenta in channel n, and the interaction potential $V_n(r)$. The FA is the antisymmetrized projection of the parent wave function (WF) $\left|\Psi_k\right\rangle$ on the channel WF $\left|n\right\rangle=\left|\left[\Phi_D(\eta_1)\Phi_p(\eta_2)Y_{lm}(\hat{r})\right]_n\right\rangle$:

$$I_n^k(r)=r\left\langle\Psi_k\left|\mathcal{A}\left\{\left[\Phi_D(\eta_1)\Phi_p(\eta_2)Y_{lm}(\hat{r})\right]_n\right\}\right\rangle\right. \tag{4}$$

where $\Phi_1(\eta_1)$ and $\Phi_2(\eta_2)$ are the internal (space-spin) wave functions of the fragments, $Y_{lm}(\hat{r})$ is the wave function of the angular motion, $\mathcal{A}$ is the inter-fragment antisymmetrizer, r connects the centers of mass of the fragments, and the symbol $\left\langle\ \middle|\ \right\rangle$ means integration over the internal coordinates and angular coordinates of relative motion. The diagonal elements V_{nn} of the potential are given by a sum of nuclear and Coulomb terms:

$$V_n(r)=V_{nn}(r)=V_0^{nucl.}(r)+V_0^{Coul.}(r) \tag{5}$$

For the nuclear potential we use the Woods-Saxon parametrization:

$$V_0^{nucl}(r)=-\frac{V_0}{1+\exp((r-R_0)/a)} \tag{6}$$

where $R_0=r_0(A_P^{1/3}+A_T^{1/3})$ and a is the diffuseness.

The Coulomb potential is taken of the usual form:

$$V_0^{Coul}(r)=\left\{\begin{array}{c}\dfrac{Z_PZ_Te^2}{2R_c}\left[3-\left(\dfrac{r}{R_c}\right)^2\right],\quad r\le R_c\\ \dfrac{Z_PZ_Te^2}{r},\quad r>R_c.\end{array}\right\} \tag{7}$$

with $R_c=r_c(A_P^{1/3}+A_T^{1/3})$.

The equations (2, 3) are solved with usual boundary conditions for the decay problem:

$$u_n^0(r\longrightarrow 0)=0;\quad u_n^0(r\to\infty)\to i/2(k_n/\pi Q_n)^{1/2}\{u_n^{(-)}(r)+S_n u_n^{(+)}\} \tag{8}$$

$$u_n^{\nu}(r\longrightarrow 0)=0;\quad u_n^{\nu}(r\to\infty)=0 \tag{9}$$

where $\hbar k_n=(2mQ_n)^{1/2}$, S_n is the scattering amplitude, $u_n^{(\pm)}(r)=G_n(r)\pm iF_n(r)$ and F_n and G_n are the regular and irregular Coulomb functions. The lower limit in integrals (1) is an arbitrary small radius $r_{min}>0$, while the upper limit r_{max} is close to the first exterior node of $u_n^0(r)$. To avoid the usual ambiguities encountered in formulating the potential for the resonance tunneling of the spherical barrier we iterate directly the nuclear potential in equations of motion [14]. The "one-body" (o.b.) resonance width in the single channel problem can be expressed only with the eigenvalues and eigenfunctions of the system:

$$\Gamma_n^{o.b.}=2\pi\left|\frac{\int_{r_{\min}}^{r_{\max}}G_n(r)u_n^0(r)dr}{\int_{r_{\min}}^{r_{\max}}G_n(r)u_n^{o.b.}(r)dr}\right|^2. \tag{10}$$

where $u_l^{o.b.}(r)$ is a solution of Eq. (3) in which $I_n^k(r)$ is merely replaced by $G_n(r)$.

3.2. COUPLED CHANNELS

The relative motion of the fragments can be strongly influenced by couplings of the relative motion of the fragments to several nuclear intrinsic motions. The usual way to address the effects of coupling between the intrinsic degrees of freedom and relative motion is to numerically solve the coupled channel equations, including all the relevant channels. The total decay width for the multichannel decay of the state k into a set of $\{n\}$ different channels is [15]:

$$\Gamma^k=\sum_n\Gamma_n^k,\qquad \text{where:} \tag{11}$$

$$\Gamma_n^k=2\pi\left|\frac{\int_{r_{\min}}^{r_{\max}}I_n^k(r)u_n^0(r)dr}{\int_{r_{\min}}^{r_{\max}}I_n^k(r)u_n^k(r)dr}\right|^2. \tag{12}$$

In Eq. (9) $I_n^k(r)$ is the particle (cluster) formation amplitude (FA) and $u_n^k(r)$ and $u_n^0(r)$ are the solutions of the systems of differential equations

$$\left[\frac{\hbar^2}{2m}\left(\frac{d^2}{dr^2}-\frac{l(l+1)}{r^2}\right)-V_{nn}(r)+Q_n\right]u_n^0(r)+\sum_{m\neq n}V_{nm}(r)u_m^0(r)=0 \tag{13}$$

$$\left[\frac{\hbar^2}{2m}\left(\frac{d^2}{dr^2}-\frac{l(l+1)}{r^2}\right)-V_{nn}(r)+Q_n\right]u_n^{\nu}(r)+\sum_{m\neq n}V_{nm}(r)u_m^{\nu}(r)=I_n^{\nu}(r) \tag{14}$$

The matrix elements V_{nm} of the coupling Hamiltonian consist also of nuclear and Coulomb components. The nuclear component can be generated by changing the target radius in the nuclear potential to a dynamical operator

$$R_0 \to R_0+\hat{O}=R_0+\beta_2 R_T Y_{20}+\beta_4 R_T Y_{40} \tag{15}$$

where $R_T=r_0A_T^{1/3}$ and β_2, β_4 are the quadrupole and hexadecapole deformation parameters of the deformed target nucleus, respectively. The nuclear coupling term is thus given by

$$V^{nucl}(r,\hat{O})=-\frac{V_0}{1+\exp((r-R_0-\hat{O})/a)}. \tag{16}$$

The resulting nuclear coupling matrix elements between states $|n\rangle=|I0\rangle$ and $|m\rangle=|I'0\rangle$ are

$$\begin{aligned}V_{nm}^{nucl.}(r)&=\langle I0|V^{nucl.}(r,\hat{O})\langle I'0|-\delta_{nm}V_0^{nucl.}(r)=\\&=\langle\alpha|I0|\alpha\rangle\langle\alpha|I'0\rangle V^{nucl.}(r,\lambda_\alpha)-\delta_{nm}V_0^{nucl.}(r);\end{aligned} \tag{17}$$

$$\hat{O}_{II'}=\left[\frac{5(2I+1)(2I'+1)}{4\pi}\right]^{1/2}\beta_2R_D\left(C_{000}^{I2I'}\right)^2 \tag{18}$$

$$+\left[\frac{9(2I+1)(2I'+1)}{4\pi}\right]^{1/2}\beta_4R_D\left(C_{000}^{I4I'}\right)^2. \tag{19}$$

Similarly, the Coulomb matrix elements are then given by

$$\begin{aligned}V_{nm}^{Coul.}(r)=&\frac{3Z_DZ_pR_D^2}{5r^3}\left[\frac{5(2I+1)(2I'+1)}{4\pi}\right]^{1/2}\left(\beta_2+\frac{2}{7}(5/\pi)^{1/2}\beta_2^2\right)\left(C_{000}^{I2I'}\right)^2\\&+\frac{3Z_DZ_pR_D^2}{9r^5}\left[\frac{9(2I+1)(2I'+1)}{4\pi}\right]^{1/2}\left(\beta_4+\frac{9}{7}\beta_2^2\right)\left(C_{000}^{I4I'}\right)^2.\end{aligned} \tag{20}$$

In the case in which all exit channels are open the boundary conditions should be:

$$\begin{aligned}&u_n^0(r\to0)=0;\\&u_n^0(r\to\infty)\to i/2(k_n/\pi Q_n)^{1/2}\left\{\delta_{nm}\exp\left[-i(k_n-l\pi/2)\right]-S_{nm}\exp\left[i(k_nr-l\pi/2)\right]\right\}\end{aligned} \tag{21}$$

$$u_n^{\nu}(r\to0)=0;\qquad u_n^{\nu}(r\to\infty)=0 \tag{22}$$

where S_{nm} is the scattering matrix. The solutions $u_n^0(r)$ may be matched to the boundary conditions at two values of r large enough so the terms V_{nm} are negligible. A special type of eigenvalue solution will be considered here for which the behavior of solution in each separate channel is similar to that of G_n in the one channel problem.

The present analysis of nuclear decay rates is based on the following key points: the shell model and resonance treatment of cluster formation amplitudes, account the couplings between the relative motion of the fragments and several nuclear collective motions, account the effects of non-linear couplings to all orders, self-consistence of the scattering potential, the rotational excitation of nuclei by the cluster transfer and the existence and convergence of the resonance scattering solution. Such an analysis includes the most important aspects of nuclear structure and reaction dynamics and permits to derive conclusions concerning basic nuclear properties mass, spins, momenta, lifetimes.

4. DETAILS OF THE CALCULATIONS

4.1. CLUSTER FORMATION AMPLITUDE (CFA)

Our goal is to make microscopic (shell model) estimations for α-decay rates at the SHEs whose nuclear structure has been investigated extensively in microscopic approaches such as Skyrme Hartree-Fock (SHF) theory and Relativistic Mean-Field (RMF) theory or Macroscopic-Microscopic (MM) method. The most notable success of the MM approach has been the Finite-Range Droplet Model (FRDM) which allows to identify the major magic numbers in the region of SHEs. The FRDM predicts a magic proton number at $Z = 114$, while experimental data give litle support to this magic number. All these approaches use the Strutinsky shell correction method for the microscopic single-particle shell model components. To explore the occurrence of a magic number in the region of SHEs, extensive shell-corrections calculations have been performed by Kruppa [21] *et al.* for a set of RMF and Skyrme forces. The contrasting difference between the behaviour of s.p. spectra and of magic numbers can be attributed to the quite different shell structure in SHF and RMF approaches [15]. In the present paper we have calculated microscopically the α-CFA using the single particle wave functions extracted from self-consistent calculations of Kruppa [21]. In this purpose we use the method which has been first developed by Mang and Rasmussen [3, 4], for the harmonic oscillator s.p. wave functions and later extended to Woods-Saxon wave functions [11, 17, 18]. Following [17] we use two kinds of FAs: the shell model FAs given on the basis of shell model s.p. wave functions, and the one-body resonance amplitude [14] that results by using

procedure. In the first case using in Eq. (4) shell model w.f. (see below) one obtains a shell model estimation of formation amplitude $I_n^k(r)$ and from Eq. (1) a shell model width Γ_n^k. In the second case we obtain the asymptotic formation amplitude $I_n^{o.b.}(r) \cong G_n(r)$ and from Eq. (8) $\Gamma_n^{o.b.}$. The CFA defined in $Ec(x)$ is simply related to the amplitude of reduced width [17, 22, 12]:

$$\gamma_n^k(r) = (\hbar^2/2mr)^{1/2} I_n^k(r). \tag{23}$$

The ratio

$$S_n^k = \Gamma_n^k/\Gamma_n^{o.b.} = T_n^{o.b.}/T_n^k \tag{24}$$

is a structure factor, a measure of global contribution of shell effects, finite sizes of nucleons and α-particle to the one-body width approximation (where α is a pointlike particle and all these effects are neglected). For the deformed SHEs the shell corrections are extracted in [21] using the standard Strutinsky method in which the positive energy spectrum has been approximated by quasibound resonance states. Actually, in our second case we extract the asymptotic CFA exactly from the same spectrum of quasibound resonance states [53, 17]. For the inverse of decay reactions or cluster transfer reactions the factor S_n^k provides similar information [22, 12]. According to the shell model of the nucleus the w. f. of an individual nucleon in the self-consistent field can be represented in the form of a product of a space function, a spin function and an isospin function:

$$\psi_\alpha(i) = R_{nlm}(r_i)\chi_\mu(\sigma_i)t_\nu(\tau_i)$$

where m is the orbital-angular momentum component, μ and ν is the spin and isospin components and α denotes the set of quantum numbers (α = n, l, m, μ, ν). The wave function of a system of A nucleons is represented in the form of a product of A one-particle w.f. (with space, spin and isospin components), which, however, should be antisymmetrized with respect to interchanges of any pair of nucleons. This antisymmetrization will be achieved if we write the w.f. of the system of A nucleons in the form of a Slater determinant:

$$\Psi_{\{\alpha\}} = (A!)^{-1/2} \begin{vmatrix} \psi_{\alpha_1}(r_1) & \psi_{\alpha_1}(r_2) & . & \dots & \psi_{\alpha_1}(r_A) \\ \psi_{\alpha_2}(r_1) & \psi_{\alpha_2}(r_2) & . & \dots & \psi_{\alpha_2}(r_A) \\ . & . & . & \dots & . \\ . & . & . & \dots & . \\ \psi_{\alpha_A}(r_1) & \psi_{\alpha_A}(r_2) & \dots & \dots & \psi_{\alpha_A}(r_A) \end{vmatrix}$$

where {α} denotes the set of quantum numbers of the occupied one-particle (shell model) states. In the shell model case we simply put in Eq. (4) $|\Psi_k\rangle = \Psi_{\{\alpha\}} = (A!)^{-1/2} \det \| \Psi_{\{\alpha_i\}}(r_i) \|$, $i = 1, A$. As discussed in [21, 19, 20] the main factors

that influence the single-proton shell structure of SHEs are *i)* the Coulomb potential and *ii)* the spin-orbit splitting. As far as the protons are concerned, the important spherical shells are the closely spaced 1i13/2 and 2f7/2 levels which appear just below the $Z = 114$ gap, the 2 f 5/2 shell which becomes occupied at $Z = 120$, the 3p3/2 shell which becomes occupied at $Z = 124$, and the 3p1/2 and 1i11/2 orbitals whose splitting determines the size of the $Z = 126$ magic gap. The ordering of single-proton states is practically the same for all the self-consistent approaches with realistic effective interactions, their relative positions depend on the choice of force parameters. Since in the region of SHEs the single-particle level density is relatively large, small shifts in positions of single-particle levels can influence the strength of single-particle gaps and be crucial for determining the shell stability of a nucleus. While most macroscopic-microscopic non-self-consistent approaches predict $Z = 114$ to be magic, self-consistent calculations suggest that the center of the proton shell stability should be moved up to higher proton numbers, $Z = 120$, 124, or 126. It is to be noted that the Coulomb potential mainly influences the magnitude of the $Z = 114$ gap. Here, the self-consistent treatment of the Coulomb energy is a key factor. On the other hand, the spin-orbit interaction determines the position of the 2f and 3p shells which define the proton shell structure above $Z = 114$. The spherical neutron shell structure is governed by the following orbitals: 1j15/2 below the $N = 164$ gap, 2g7/2, 3d5/2, 3d3/2, 4s1/2, and 1 j13/2 whose splitting determines the size of the $N = 184$ spherical gap. Again, similar to the proton case, the order of the single-neutron orbitals between $N = 164$ and 184 is rather robust, while the sizes of single-particle gaps vary. For instance, the $N = 172$ gap, predicted by the RMF calculations, results from the large energy splitting between the 2g7/2 and 3d5/2 shells. A new method of calculating the shell correction, based on the correct treatment of resonances, has been developed [17, 14]. The improved method is based on the theory of Gamow states eigenstates of a one-body Hamiltonian with purely outgoing boundary conditions which can be calculated numerically for commonly used optical-model potentials. Present Skyrme-Hatree-Fock (SHF) and Relativistic Mean Field (RMF) calculations with realistic effective forces are able to describe s.p. nuclear properties with an accuracy which is comparable to that obtained in more phenomenological macroscopic-microscopic models based on the shell correction method. Such calculations offer us a starting point in the treatmement of the nucleon clustering around the particle threshold by using the single-particle level density in the presence of a low-lying proton continuum.

4.1.1. Eigenvalue finding

To propagate the solution of homogeneous system (11) in the interval $[r_{min}, r_{max}]$ we used the routine DOPRIN [54]. This routine gives the numerical solution of a system of second order ordinary differential equations of the form

$y'' = f(x, y)$. It is based on an embedded Runge-Kutta-Nyström method of order (6) 7 (with stepsize control) and is due to Dormand and Prince (see [54]). As said before, at the bound r_{max} the solution is a Coulomb function. It is calculated by the subroutine COULCC of Thompson and Barnett (see [55]) and is used as starting value for the backward integration. The boundary value problem has solution only for some particular values of the parameter chosen as eigenvalue (denoted by λ). In our approach this adjustable parameter is the depth of the Woods-Saxon potential (the energies are fixed). For some input λ the solution is propagated in two directions, from r_{min} up to the matching point r_m, and from r_{max} up to the same r_m. is a linear combination of n linear independent solutions.

5. RESULTS

Aiming at confirmation of a part of recent results [30] for the decay chain of $^{294}118$ and $^{290–291}116$ we estimate the α-decay rates using the shell model formation and resonance reaction amplitudes given by selfconsistent models for nuclear structure and low-energy dynamics. For calculating T_α and S_α we use the s.p. shell model states [20, 21] shown in Figs. 1–2, (protons: $1i_{13/2}$, $2f_{7/2}$, $3p_{3/2}$, neutrons: $2g_{7/2}$, $3d_{5/2}$, $3d_{5/2}$), the deformation parameters [44], the measured [30] $E_\alpha^{\text{exp.}}$ for $^{294}118$, $^{290}116$, $^{286}114$ and calculated ones [31–35] for $^{282}112$. Fig. 3 shows [30] the three α-chains originated from the even-even isotope $^{294}118$ ($E_\alpha = 11.65 \pm 0.06$ MeV, $T_\alpha = 0.89^{+1.70}_{-0.31}$ ms) produced in the 3n-evaporation

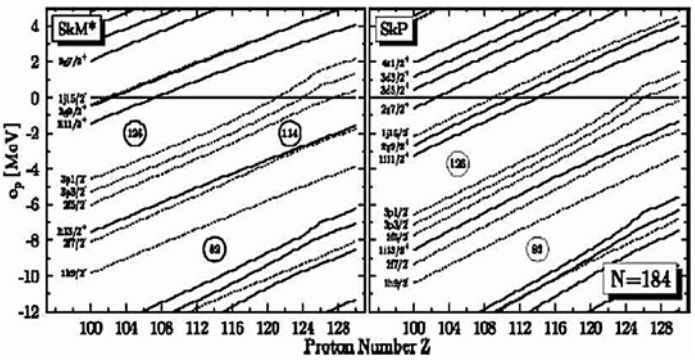

Fig. 1 – Single-proton Fermi levels of the parent and daughter nuclides with $Z = 118–106$ used in (Eq. 4) for calculating the shell-model overlap integrals $I_n^k(r)$. Single-proton levels isotopes are obtained [21] in the RMF approach for $160 \le N \le 190$ with NL3 (left) and NL-Z2 no linear parameterizations.

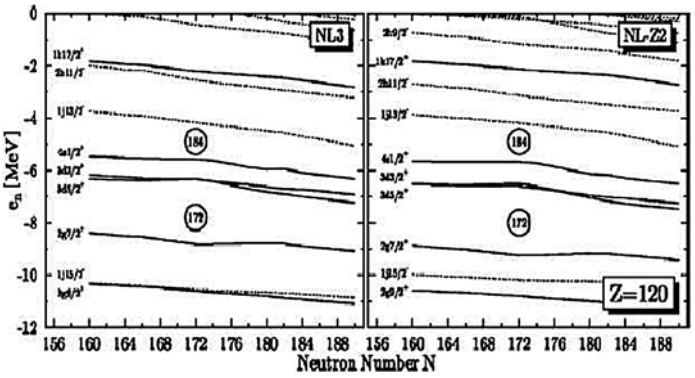

Fig. 2 – Single-neutron Fermi levels of the parent and daughter nuclides [21] used in calculating the overlap integrals $I_n^k(r)$ (Eq. 4) for the nuclides with $Z = 118$–106. The levels for $N = 184$ isotones with $110 < Z < 130$ are obtained with Skyrme-Hartree-Fock model with SKN (left) and SKP effective interactions. Positive (negative) parity levels are indicated by solid (dashed) lines and by their spherical labels (nlj). In both cases the nucleus $Z = 126$ is proton unbound.

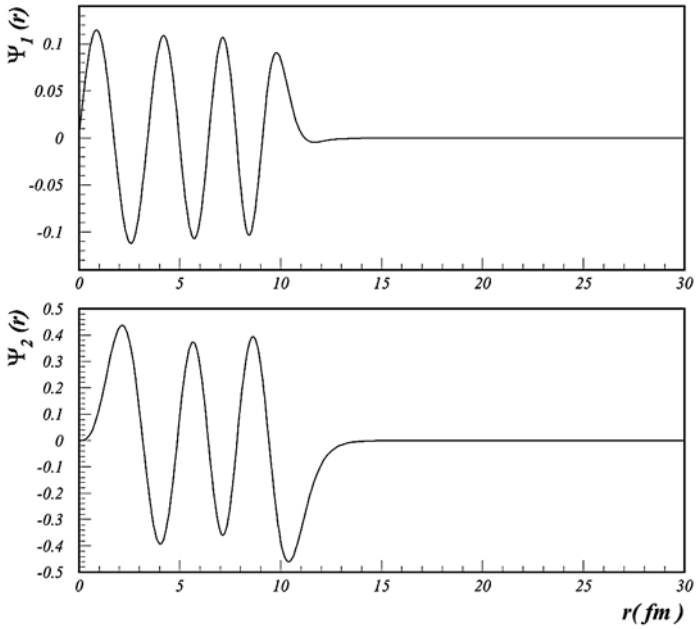

Fig. 3 – The eigen solutions of the coupled channel Schrödinger equation for two channel decay of ^{273}Dt [27].

channel of the ^{249}Cf + ^{48}Ca reaction with a maximum cross section of $0.5^{+1.6}_{-0.3}$ pb. Our results are shown in Tables 1–3 and figs. 4–6, for ^{294}118, ^{290}116 and ^{286}114.

Table 1

Eigenvalue calculation

n	λ_n	δ_n	$\Phi(\lambda_n)$
1	51.118656066184	–1.11866D+00	9.54516D–01
2	50.925660698315	1.92995D–01	–2.21707D+00
3	50.944061874603	–1.84012D–02	2.63291D–01
4	50.944255654746	–1.93780D–04	2.71568D–03
5	50.944255675946	–2.11993D–08	2.97027D–07
6	50.944255675943	2.99123D–12	–4.19106D–11

Table 2

Decay properties of nuclei produced by Yu. Ts. Oganessian *et al.* [30]

Nuclide	Decay mode	Q_α [MeV]	$T^\alpha_{1/2}$ [s] Empiric estimates[a]		$T^\alpha_{1/2}$ [s] Microscopic calculations		S^k_n
			Ref. [30] Q_α	This work $Q_\alpha + E_{scr}$	Shell model[b] $Q_\alpha + E_{scr}$	Superfl. model[c] $Q_\alpha + E_{scr}$	
^{294}118	α	11.81 ± 0.07	$0.89^{+1.07}_{-0.31}$ ms	$0.48^{+0.21}_{-0.15}$ ms	$0.72^{+1.98}_{-0.27}$ ms	$.13^{+.49}_{-.35}$ ms	$.410^{-3}$
^{290}116	α	10.95 ± 0.09	$7.1^{+3.2}_{-1.7}$ ms	$15.15^{+10.50}_{-6.14}$ ms	21^{+16}_{-8} ms	$2.68^{+1.83}_{-1.08}$ ms	$.210^{-3}$
^{286}114	α	10.18 ± 0.09	$0.13^{+0.04}_{-0.02}$ s	$0.40^{+0.31}_{-0.13}$ s	$0.28^{+0.17}_{-0.13}$ s	$0.02^{+0.01}_{-0.01}$ s	$.110^{-2}$
^{282}112	α, *SF*	10.25 ± 0.25[d]		$60.49^{+231.90}_{-47.25}$ ms	$40.8^{+154.2}_{-31.92}$ ms	$3.23^{+11.73}_{-2.49}$ ms	$.510^{-3}$

[a] Viola-Seaborg formula [41] with parameters [42, 43].
[b] Shell-model formation amplitude [5, 17].
[c] Superfluid model formation amplitude [36].
[d] The limit values include all the predictions:[31–35].

Table 3

Decay properties of nuclei produced by Yu. Ts. Oganessian *et al.* [30]

Nuclide	Decay mode	Q_α [MeV]	$T^\alpha_{1/2}$ [s] Empiric estimates[a]		$T^\alpha_{1/2}$ [s] Microscopic calculations		S^k_n
			Ref. [30] Q_α	This work $Q_\alpha + E_{scr}$	Shell model[b] $Q_\alpha + E_{scr}$	Superfl. model[c] $Q_\alpha + E_{scr}$	
^{290}116	α	11.0 ± 0.08	$7.1^{+3.2}_{-1.7}$ ms	$11.34^{+6.7}_{-4.18}$ ms	$12.70^{+6.9}_{-10.4}$ ms	$12.34^{+7.0}_{-4.4}$ ms	.20
^{286}114	α, *SF*	10.33 ± 0.06	$0.13^{+0.04}_{-0.02}$ s	$0.15^{+0.07}_{-0.04}$ s	$0.14^{+0.17}_{-0.01}$ s	$0.10^{+0.05}_{-0.03}$ s	.17

[a] Viola-Seaborg formula [41] with parameters [42, 43].
[b] Shell-model formation amplitude [5, 17].
[c] Superfluid model formation amplitude [36].

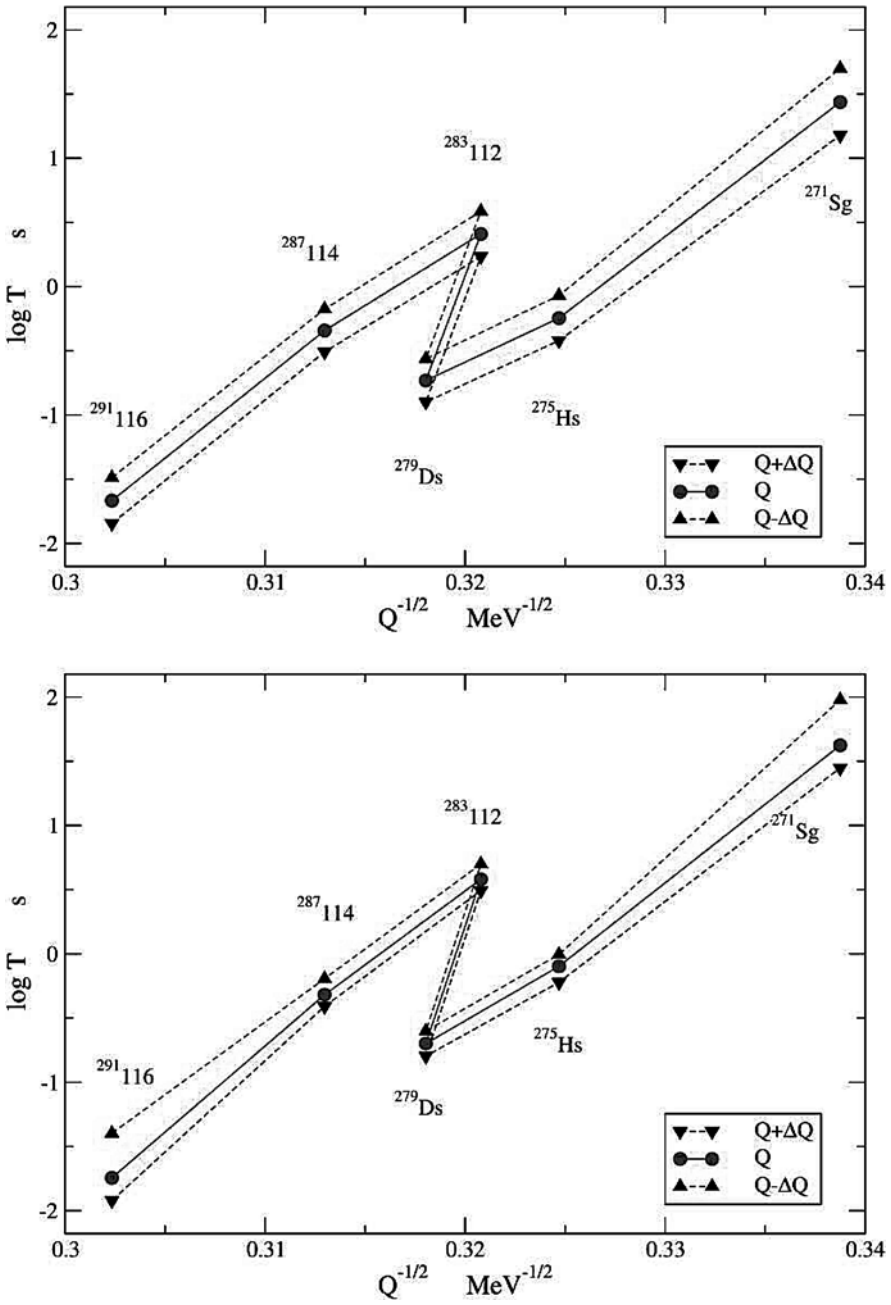

Fig. 5 – The Gamow plot of calculated for α-halflives of $^{291}116$ observed in the $^{249}Cf + ^{48}Ca$ reactions [30]. The upper plot shows our results, while the lower one presents the Viola-Seaborg empirical estimates. The measured α-particle energies are taken from [30].

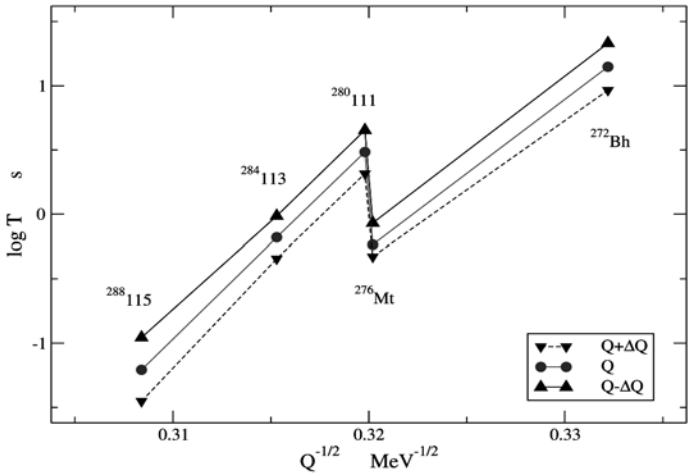

Fig. 6 – The Gamow plot for calculated α-halflives for the element ^{288}115 and its α-descendants. (down triangles correspond to $Q + \delta Q$, up triangles to $Q - \delta Q$ and circles to Q values [29]).

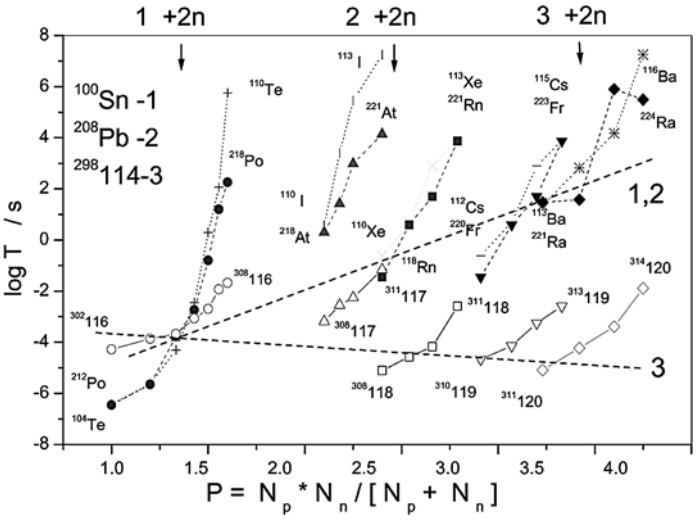

Fig. 7 – Experimental α-halflives of the trans-tin(1) and the trans-lead(2) nuclei and the calculated α-halflives for the trans-^{298}114 nuclei *versus* Casten-Zamfir factor $P = N_p * N_m / (N_p + N_n)$.

we can observe a reasonable agreement with estimates [30]. Also for branching ratios α/*SF* for ^{286}114 and ^{282}112 nuclei we observe agreement with data. For Q_α estimates [37–40], the α-channel of ^{282}112 practically disappears. The difference in the magnitude of the halflives between present and previous predictions [45–52],

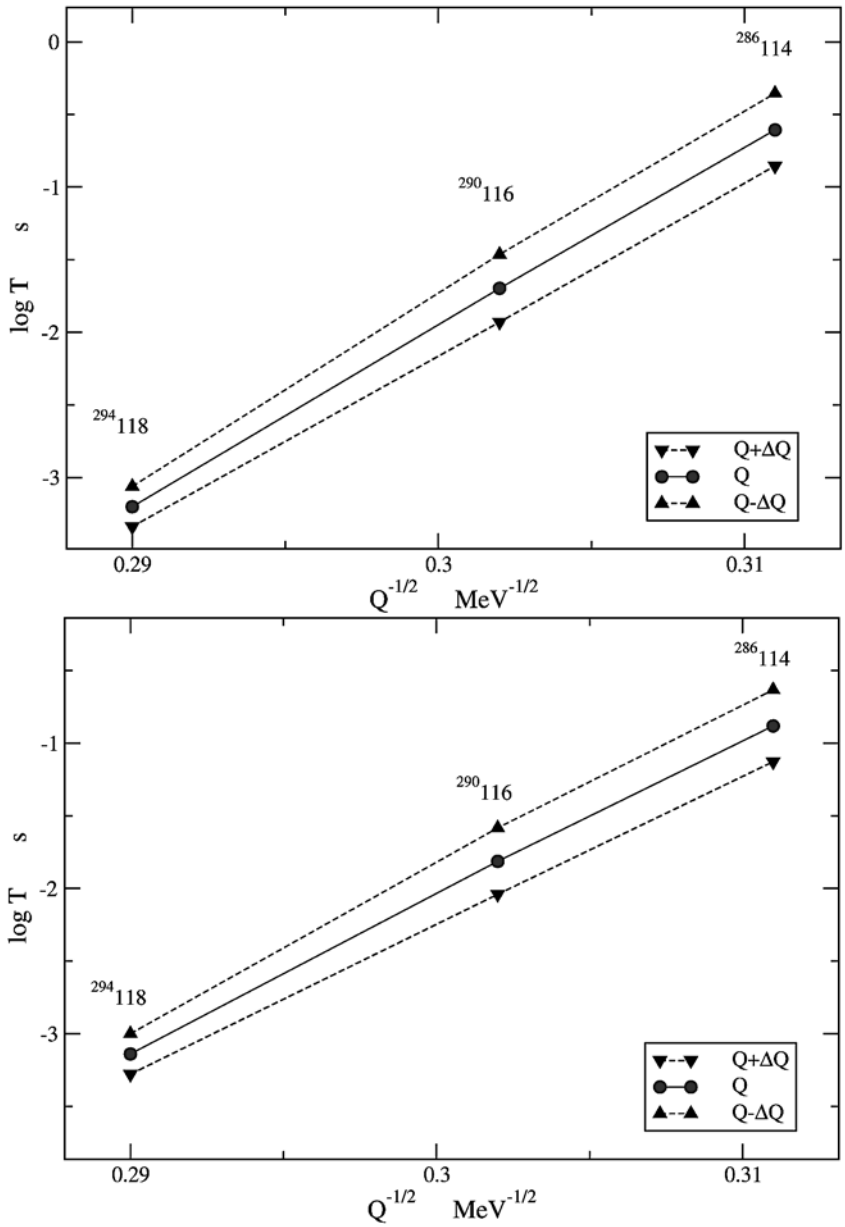

Fig. 8 – Experimental α-halflives of the trans-tin(1) and the trans-lead(2) nuclei and the calculated α-halflives for the trans-^{298}114 nuclei *versus* Casten-Zamfir factor $P = N_p * N_m / (N_p + N_n)$.

indicate the strong influence of the proton shell at $Z \geq 118$. Theoretical results for the all observed alpha channels are given in Tables 1–3 and are pictured in Figs. 4–6.

The calculated α-half-lives being much shorter than the expected fission half-lives are of physical significance and interest. In most cases our α-half-time estimates are in excellent agreement with the existing data and differ from the empirical predictions given by the Viola-Seaborg formula. In most cases, the decay rates predicted agree well with the measured data. Systematic calculations of spectroscopic properties of SHEs have become feasible, as has been shown on the example of ground states of $^{294}118$ and its α-descendants. The agreement with experiment supports the basic correctness of our unified picture for heavy-ion and α-resonances and gives us some guaranty for reasonable predictions to the nuclides with $Z > 114$ just above the magic shell $Z = 114$ and $N = 184$.

6. SUMMARY AND OUTLOOK

In this work we develop a general method for estimating the absolute α-emission rates of ground and excited states of nuclei by solving the radial Schrödinger equation for coupled channels problem with outgoing asymptotics and resonance conditions. The method allows us to perform detailed tests of current theoretical models for the nuclear structure and α-decay modes since the decay rates are the wavefunction sensitive quantities in which both the resonant and nonresonant continuum are taken properly into account. All these probes reveal the crucial details nedeed to certify a theoretical description of the structure and dynamics of a particular nuclide. Characterized by their emission rates the decay of a nuclear state can be enhanced due to the collective behavior or forbidden by internal selection rules. We calculated in different approximations the α -half-lives of nuclides $^{294}118$, $^{290–291}116$ and their alpha descendants using the measured emission energies, shell model and one-body formation amplitudes and reaction amplitude for resonance tunneling.

Fine structure (FS) manifests in many features, *e.g.*, in ground state properties like half-life, radius and deformation and binding energy. Analysing the measured energy levels and fine structure in alpha decay of SHEs, two important aspects emerged:

1) the SHEs with double magic shells are exceptionally strongly bound, while the reaction decay energies are appreciablly reduced,

2) compared to other even-even closed shell nuclei the superheavy nuclei which are small multiples of α-particles built from valence protons and neutrons have extremly large Q_α values, and therefore the α-decay is expected to be the dominant decay mode for nuclei above the double magic shells.

Our study reveals a close connection between particle decay properties and the number of valence nucleons. The valence nucleon number appears as a dominant controlling factor in the evolution of α-decay properties, and therefore, it was possible to devise some observables related to it which describe the systematic

and periodic variations in the structure and basic decay properties. The following conclusions can be drawn from our study:

1) The spin-parity and emission energy information can be accurately extended, with support from theoretical investigations, from the daughter to parent (unknown). Thus, the decay chain can be rebuilt from the bottom and this helps to identify new nuclides through their α-decay characteristics and measured α-α, parent-daughter space-time correlations.

2) The nuclides just above $Z = 114$ and $N < 184$ are predicted to be prominent α-emitters, with the shortest α-half-lives in the range of tens of ms.

3) The nuclear decay properties (emission energies and half-lives) of the studied nuclei appear as a periodic function of the number of valence nucleons. An α-periodicity can be observed in the evolution of the decay properties with the number of valence nucleons. Therefore, it was possible to deduce the properties of nuclides above $Z = 114$ from what we know in the $Z = 82$ and $Z = 50$ regions by using the symmetry arguments associated to the α-periodicity.

Acknowledgements. We thank Professors Yu. Ts. Oganessian, V. K. Utynkov, S. Hofmann, G. Münzenberg, W. Scheid, S. Misicu, A. Sandulescu for many stimulating discussions. This work was supported from Contract CEEX05-D08-10.

REFERENCES

1. T. Teichmann, E. P. Wigner, Phys. Rev., **79**, 30 (1952).
2. R. G. Thomas, Prog. Theor. Phys., **12**, 253 (1954).
3. H. J. Mang, Phys. Rev., **119**, 1069 (1960).
4. H. J. Mang, J. O. Rasmussen, Kgl. Danske Videnscab Selskab, Mat. Fys. Skifter 2, **3** (1962).
5. H. J. Mang, Ann. Rev. Nucl. Sci., **14** (1984).
6. G. Breit, Encyclopedia of Physics, Vol. XLI, Nuclear Reactions II: Theory, Springer-Verlag, 1959 (Ed. S. Flugge).
7. H. Feshbach, Ann. Phys. 5 (NY), **357** (1958).
8. K. Harada, E. A. Rauscher, Phys. Rev., **169**, 818 (1968)).
9. S. G. Kadmensky, V. E. Kaletchis, Yad. Fiz., **12**, 70 (1970).
10. J. Schlitter, Nucl. Phys., A211, **96** (1973).
11. A. Sandulescu, I. Silisteanu, R. Wuensch, Nucl. Phys., A305, **205** (1978).
12. P. E. Hodgson, E. Betak, Phys. Rep., **374**, 89 (2003).
13. I. Silișteanu, W. Scheid, A. Sandulescu, Nucl. Phys., **A679**, 317 (2001).
14. I. Silișteanu, W. Scheid, Phys. Rev., **51**, 2023 (1995).
15. I. Silișteanu, W. Scheid, A. O. Silișteanu, Rom. Rep. Phys., **57**, 4 (2005).
16. K. Hagino, N. Rowley, A. T. Kruppa, Comp. Phys. Commun., **123**, 143 (1999).
17. I. Silișteanu, Preprint E4-80-8, JINR, Dubna (1980).
18. V. I. Furman, S. Holan, G. Stratan, Nucl. Phys., **A239**, 114 (1975).
19. S. Cwiok, J. Dobaczevski, P.H-H. Heenen, P. Magierki, W. Nazarewicz, Nucl. Phys., **A611**, 211 (1996).
20. M. Bender, K. Rutz, P.-G. Reinhard, J. A. Maruhn, W. Greiner, Phys. Rev., **C60**, 034304 (1999).
21. A. T. Kruppa *et al.*, Phys. Rev., **C61**, 034313 (2000).

22. R. G. Lovas *et al.*, Phys. Rep., **294**, 265 (1998).
23. D. Robson, Nucl. Phys., **A204**, 204 (1973).
24. R. S. Simon *et al.*, Z. Phys., **A325**, 197 (1986).
25. P. Reiter *et al.*, Phys. Rev. Lett., **82**, 509 (1999).
26. S. Hofmann *et al.*, Zeit. Phys., **A354**, 229 (1996).
27. S. Hofmann, G. Münzenberg, Rev. Mod. Phys., **72**, 733 (2000).
28. Yu. Ts. Oganessian *et al.*, Phys. Rev., **C69**, 021601 (2004).
29. Yu. Ts. Oganessian *et al.*, Phys. Rev., **C69**, 054607 (2004).
30. Yu. Ts. Oganessian *et al.*, Phys. Rev., **C74**, 044602(2006).
31. S. Goriecly *et al.*, Phys. Rev., **C66**, 024326 (2002).
32. S. Typel, B. A. Brown, Phys. Rev., **C67**, 034313 (2003).
33. J. F. Berger, D. Hirata, M. Girod, Acta Phys. Pol., **B34**, 1909 (2003).
34. S. Cwiok, P. H. Heenen, W. Nazarewicz, Nature, **433**, 705 (2005).
35. M. Warda *et al.*, Intern. J. Mod. Phys., **E15** (in press).
36. F. Barranco, R. A. Broglia, G. F. Bertrech, Phys. Rev. Lett., **60**, 507, (1988).
37. I. Muntian, Z. Patyk, A. Sobiczewski, Phys. At. Nucl., **66**, 1015 (2003).
38. A. Baran *et al.*, Phys. Rev., **C72**, 044310 (2005).
39. Y. K. Gambhir, A. Bhagwat, M. Gupta, Phys. Rev., **C71,** 037301 (2005).
40. M. Bender *et al.*, Phys. Rev., **C61**, 031302 (2000).
41. V. E. Viola, G. T. Seaborg, J. Inorg. Nucl. Chem., **28**, 741 (1966).
42. A. Sobiczewsky, Z. Patyk, S. Cwiok, Phys. Lett., **B 224**, 1 (1989).
43. Z. Patyk, A. Sobiczewski, Nucl. Phys., **A354**, 229 (1996).
44. P. Möller *et al.*, At. Data and Nucl. Data Tab., **66**, 131 (1997).
45. V. Yu. Denisov, H. Ikezoe, Phys. Rev., **C72**, 064613 (2005).
46. P. Mohr, Phys. Rev., **C73**, 031301 (2006).
47. P. Roy Chowdhury, C. Samanta, D. N. Basu, Phys. Rev., **C73**, 014612 (2006).
48. Chang Xu, Zhongzhou Ren, Phys. Rev., **C74**, 014304 (2006).
49. Takatoshi Ichikawa *et al.*, Phys. Rev., **C71**, 044608 (2005).
50. I. Silisteanu *et al.*, Proc. CSSP-2005 Exotic nuclei and Nuclear/ Particle Astrophysics (World Scientific, 2006, Eds. Stoica, Trache, Tribble) p. 423.
51. S. G. Nilsson *et al.*, Phys. Lett., **B28**, 458 (1969); Nucl. Phys. **A131** (1969), Nucl. Phys. **A115**, 545 (1968).
52. E. O. Fiset, J. R. Nix, Nucl. Phys., **A193**, 647 (1972).
53. M. Rizea, Comp. Phys. Commun., **143**, 83–99 (2002).
54. E. Hairer, S. P. Norsett, G. Wanner, Springer Verlag, Berlin (1987).
55. I. J. Thompson, A. R. Barnett, Comput. Phys. Commun. **36**, 363–372 (1985).
56. K. Hagino, N. Rowley, A. T. Kruppa, Comp. Phys. Commun., **123**, 143–152 (1999).

Table 4

Decay properties of nuclei produced by Yu. Ts. Oganessian *et al.* [30]

Nuclide	Decay mode	Q_α [MeV]	$T^\alpha_{1/2}$ [s] Empiric estimates[a]		$T^\alpha_{1/2}$ [s] Microscopic calculations		S^k_n
			Ref. [30] Q_α	This work $Q_\alpha + E_{scr}$	Shell model[b] $Q_\alpha + E_{scr}$	Superfl. model[c] $Q_\alpha + E_{scr}$	
$^{291}116$	α	10.89 ± 0.07	$18^{+22}_{-6}10^{-3}$	$21^{+11}_{-7}10^{-3}$	$27^{+14}_{-5}10^{-3}$	$1.12^{+5.5}_{-3.6}10^{-3}$	0.9110^{-2}
$^{287}114$	α	10.16 ± 0.06	$0.48^{+0.16}_{-0.09}$	$0.45^{+0.21}_{-0.14}$	$0.62^{+0.2}_{-0.19}$	$16.18^{+4.23}_{-5.01}10^{-3}$	0.5610^{-2}
$^{283}112$	α	9.67 ± 0.06	$3.8^{+1.2}_{-0.2}$	$2.56^{+1.29}_{-0.85}$	$3.95^{+1.85}_{-1.11}$	$59.12^{+18.25}_{-24.02}10^{-3}$	0.3010^{-2}
$^{279}110$	α, *SF*	9.84 ± 0.06	$0.2^{+0.05}_{-0.04}$	$0.18^{+0.09}_{-0.16}$	$0.10^{+0.06}_{-0.03}$	$8.17^{+3.76}_{-2.55}10^{-3}$	0.1710^{-2}
$^{275}108$	α	9.44 ± 0.06	$0.19^{+0.22}_{-0.07}$	$0.56^{+0.29}_{-0.19}$	$0.26^{+0.15}_{-0.08}$	$25.41^{+12.66}_{-8.17}10^{-3}$	0.1919^{-1}
$^{271}106$	α, *SF*	8.67 ± 0.08	114^{+144}_{-36}	$27.33^{+22.68}_{-12.28}$	68^{+51}_{-22}	$1.373^{+1.119}_{-.611}$	0.410^{-2}

[a] Viola-Seaborg formula [41] with parameters [42, 43].
[b] Shell-model formation amplitude [5, 17].
[c] Superfluid model formation amplitude [36].

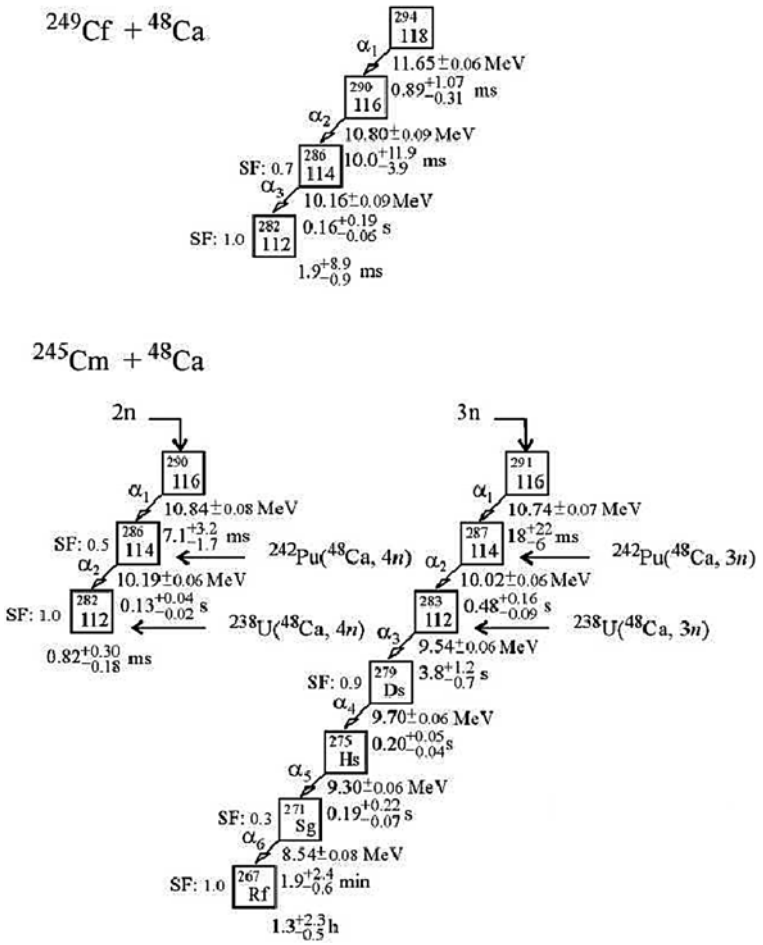

Fig. 4 – Time sequences in the decay α-chains of $^{294}118$, $^{290}116$ and $^{291}116$ observed in the $^{249}Cf + ^{48}Ca$ and $^{249}Cf + ^{48}Ca$ reactions [30]. The average measured α-particle energies, half-lives, and SF branching ratios of the observed nuclei are shown separately.